



EUROPEAN
HEMATOLOGY
ASSOCIATION



Ferrata Storti
Foundation

The *SLC40A1* R178Q mutation is a recurrent cause of hemochromatosis and is associated with a novel pathogenic mechanism

Chandran Ka,^{1,2,3*} Julie Guellec,^{1,3,4*} Xavier Pepermans,⁵ Caroline Kannengiesser,^{3,6,7} Cécile Ged,^{7,8} Wim Wuyts,⁹ David Cassiman,¹⁰ Victor de Ledinghen,¹¹ Bruno Varet,¹² Caroline de Kerguenec,¹³ Claire Oudin,⁶ Isabelle Gourlaouen,^{1,3} Thibaud Lefebvre,⁶ Claude Férec,^{1,2,7} Isabelle Callebaut¹⁴ and Gérald Le Gac^{1,2,3,7}

Haematologica 2018
Volume 103(11):1796-1805

¹UMR1078, INSERM, Université Bretagne Loire – Université de Bretagne Occidentale, Etablissement Français du Sang – Bretagne, Institut Brestois Santé-Agro-Matière, Brest, France; ²Laboratoire de Génétique Moléculaire et Histocompatibilité, CHRU de Brest, Hôpital Morvan, France; ³Laboratory of Excellence GR-Ex, Paris, France; ⁴Association Gaetan Saleun, Brest, France; ⁵Center for Human Genetics, University Hospital of St-Luc, Brussels, Belgium; ⁶UMR1149, INSERM, Centre de Recherche sur l'Inflammation, Université Paris Diderot, AP-HP, Hôpital Bichat, Département de Génétique, France; ⁷On behalf of the French National Network for the Molecular Diagnosis of Inherited Iron Overload Disorders (J. Rochette, E. Cadet, C. Kannengiesser, H. Puy, C. Ged, H. de Verneuil, G. Le Gac, C. Férec, S. Pissard, V. Gérolami), Brest, France; ⁸INSERM U1035, BMGIC, CHU de Bordeaux, Laboratoire de Biochimie et Biologie Moléculaire, France; ⁹Department of Medical Genetics, University and University Hospital of Antwerp, Edegem, Belgium; ¹⁰Department of Gastroenterology-Hepatology and Metabolic Center, University Hospital of Leuven, Belgium; ¹¹Department of Gastroenterology and Digestive Oncology, University Hospital of Bordeaux, France; ¹²Université Paris Descartes et AP-HP, Hôpital Necker, Service d'Hématologie, France; ¹³AP-HP, Hôpital Beaujon, Département d'Hépatologie, Clichy, France and ¹⁴UMR7590, CNRS, Sorbonne Universités, Université Pierre et Marie Curie-Paris, France

*CK and JG contributed equally to this work

Correspondence:

gerald.legac@univ-brest.fr

Received: January 29, 2018.

Accepted: July 6, 2018.

Pre-published: July 12, 2018.

doi:10.3324/haematol.2018.189845

Check the online version for the most updated information on this article, online supplements, and information on authorship & disclosures: www.haematologica.org/content/103/11/1796

©2018 Ferrata Storti Foundation

Material published in *Haematologica* is covered by copyright. All rights are reserved to the Ferrata Storti Foundation. Use of published material is allowed under the following terms and conditions:

<https://creativecommons.org/licenses/by-nc/4.0/legalcode>.

Copies of published material are allowed for personal or internal use. Sharing published material for non-commercial purposes is subject to the following conditions:

<https://creativecommons.org/licenses/by-nc/4.0/legalcode>,

sect. 3. Reproducing and sharing published material for commercial purposes is not allowed without permission in writing from the publisher.



ABSTRACT

Hemochromatosis type 4 is one of the most common causes of primary iron overload, after *HFE*-related hemochromatosis. It is an autosomal dominant disorder, primarily due to missense mutations in *SLC40A1*. This gene encodes ferroportin 1 (FPN1), which is the sole iron export protein reported in mammals. Not all heterozygous missense mutations in *SLC40A1* are disease-causing. Due to phenocopies and an increased demand for genetic testing, rare *SLC40A1* variations are fortuitously observed in patients with a secondary cause of hyperferritinemia. Structure/function analysis is the most effective way of establishing causality when clinical and segregation data are lacking. It can also provide important insights into the mechanism of iron egress and FPN1 regulation by hepcidin. The present study aimed to determine the pathogenicity of the previously reported p.Arg178Gln variant. We present the biological, clinical, histological and radiological findings of 22 patients from six independent families of French, Belgian or Iraqi decent. Despite phenotypic variability, all patients with p.Arg178Gln had elevated serum ferritin concentrations and normal to low transferrin saturation levels. *In vitro* experiments demonstrated that the p.Arg178Gln mutant reduces the ability of FPN1 to export iron without causing protein mislocalization. Based on a comparative model of the 3D structure of human FPN1 in an outward facing conformation, we argue that p.Arg178 is part of an interaction network modulating the conformational changes required for iron transport. We conclude that p.Arg178Gln represents a new category of loss-of-function mutations and that the study of “gating residues” is necessary in order to fully understand the action mechanism of FPN1.

Introduction

Hemochromatosis type 4 (OMIM #606069), also called ferroportin disease, is an inborn error of iron metabolism transmitted through autosomal dominant inheritance and associated with mutations in the gene encoding the solute-carrier family 40 member 1 (*SLC40A1*). Although rare, hemochromatosis type 4 is observed in different ethnic groups and is considered to be the second most common cause of hereditary iron overload after *HFE*-related hemochromatosis.^{1,2}

SLC40A1, also known as ferroportin 1 (UniProt accession number Q9NP59), is the sole iron export-protein reported in mammals. It is expressed in all types of cells that handle major iron flow, including macrophages, duodenal enterocytes, hepatocytes and placenta syncytiotrophoblasts.³ Expression of ferroportin 1 on the cell surface is predominantly regulated by the liver-derived peptide hepcidin, which induces internalization and degradation of ferroportin 1 and thereby decreases the delivery of iron to plasma.⁴ The hepcidin-ferroportin axis plays an important role in the pathogenesis of inherited and acquired iron metabolism disorders, including iron overload diseases and iron-restricted anemia.⁵

Mutations that alter ferroportin 1 function are expected to produce stronger effects in reticuloendothelial macrophages than in enterocytes or hepatocytes. These macrophages acquire most of their iron by recycling senescent red blood cells and account for >80% of the daily iron flux within the body.⁶ In line with this expectation, and at variance with *HFE*-related hemochromatosis, patients with loss-of-function mutations usually present with mesenchymal or mixed iron overload (corresponding to early iron deposition within Kupffer cells) and markedly elevated serum ferritin levels, contrasting with normal or low transferrin saturation values.^{7,8} Aggressive phlebotomy regimens can be a problem in the early stages of the disease, when patients often display borderline anemia.^{9,10}

Although a majority of *SLC40A1* mutations reported as being causally linked to hemochromatosis type 4 are true “pathogenic variants”,¹¹ there may be some doubt in the case of variants for which phenotypic, population, segregation, functional and/or computational data are lacking or not fully convincing. The problem is not specific to hemochromatosis type 4, but includes all Mendelian disorders associated with large allelic heterogeneity, and can be mimicked by non-genetic conditions.^{12,13} Assessing the pathogenicity of 18 non-synonymous *SLC40A1* variants found in 44 suspected hemochromatosis 4 patients, we previously demonstrated that eight very rare missense mutations had no noticeable effects on ferroportin 1 function or interaction with hepcidin.¹⁴ All these variants were identified in single cases showing moderate serum ferritin elevation and normal transferrin saturation, a biological condition that is common in clinical practice and is largely related to lifestyle and environmental factors.¹⁵

The present study provides strong evidence that the *SLC40A1* p.Arg178Gln missense mutation is recurrent in the *SLC40A1* gene of patients showing typical reticuloendothelial iron overload. We further demonstrate that the p.Arg178Gln ferroportin 1 mutant shows reduced ability to export iron out of the cell. This is likely a direct consequence of salt bridge disruption between Arg178 and Asp473, thereby affecting the stable formation of the

intracellular gate present in the ferroportin 1 outward facing state. Such a molecular mechanism of pathogenesis has never been reported in the context of hemochromatosis type 4.

Methods

Genetic studies

DNA was extracted from the peripheral blood of patients and unaffected family members. The complete coding sequence of *SLC40A1* and intron/exon boundaries was investigated by Sanger sequencing in the probands, while family members were only assessed for exon 6 (containing codon p.Arg178). All probands were negative for genotypes known to cause hemochromatosis types 1-3 (in the *HFE*, *HFE2*, *HAMP* and *TFR2* genes) and for mutations in the *FTL* and *BMP6* genes (hyperferritinemia cataract syndrome: OMIM#600886; hyperferritinemia without iron overload and cataract: OMIM#134790; *BMP6*-related iron overload: OMIM#112266). Polymerase chain reaction and sequencing conditions are available upon request.

A total of 734 DNA samples from healthy subjects, exclusively from north-western France (Brittany), were investigated to control the frequency of the *SLC40A1* p.Arg178Gln variant.

Informed consent for molecular studies was obtained from all patients and family members, in accordance with the Declaration of Helsinki; in line with French ethical guidelines, the Clinical Research Ethics Committee of the University Hospital of Brest approved the study on October 25, 2010.

Hepcidin measurement in human serums

Serum hepcidin concentrations were measured using liquid chromatography coupled with tandem mass spectrometry (LC-MS/MS), as previously described.¹⁶ The 95% reference interval obtained for normal hepcidin (200 serum samples from healthy subjects) ranged from 1.0 and 20.8 ng/mL (mean: 8.2 ng/mL).

Human-25 hepcidin synthesis and secretion by T-Rex-293 cells

Human *HAMP* cDNA was amplified with reverse-transcription polymerase chain reaction (RT-PCR) from total ribonucleic acid (RNA) isolated from human liver hepatocellular carcinoma HepG2 cells. The PCR product was cloned into the PCR2.1 vector using the TA Cloning Kit (Thermo Fisher Scientific), subcloned into the pcDNA4TM4/TO tetracycline-regulated mammalian expression vector (Thermo Fisher Scientific), and checked by sequencing.

T-Rex-293 cells (Thermo Fisher Scientific) were stably transfected with calcium phosphate, and colonies were selected in the presence of 1.5 µg/ml blasticidin and 100 µg/ml zeocin for four weeks. Tetracycline (Sigma, St. Louis, MO, USA) was used to induce expression of the 84 hepcidin pre-propeptide amino acids from 1.106 T-Rex-293 cells. After 48h the cell supernatant was collected, filtered through a hydrophilic nylon membrane (pore size: 0.2 µm), and measured for hepcidin-25 levels using a commercially available competitive enzyme-linked immunosorbent assay kit (ELISA; Peninsula Laboratories International, San Carlos, CA, USA). The supernatant was stored at -20°C until used.

In vitro experiments

In vitro investigations were performed as previously described^{14,17} and are presented in detail in the *Online Supplementary Data*.

3D structure modeling and analysis

Models of the 3D structure of human ferroportin 1 were built using Modeller v9.15,¹⁸ considering the sequence alignment

Table 1. Biological and clinical data of index cases and their relatives.

Family	Country	Family relationships	Gender	Age* (years)	SF (µg/L)	TS (%)	HIC (mol/g)	AST (IU/L)	ALT (IU/L)	GGT (IU/L)	CRP (mg/L)	RBC (Tera/L)	Hb (g/dL)	Ht (%)	MCV (fl)	Clinical observations	Alcohol consumption**			
1	Belgium	Index case	M	39	1873	33							15,7	45		Fatigue	Moderate			
		Father	M	61	1190									15,2	42,5					
		Daughter	F	11	322									12,6				Abstinent		
		Son	M	7	552									12,9				Abstinent		
2	France	Index case	M	55	1452	36	180	37	58	61	1.5	4.75	15.6	45,8	96,5	Digestive problems	Abstinent			
		Son	M	20	976	27	85	54	98	23	2.3	5.73	18.4	52.1	90.9	Obesity	Abstinent			
3	France	Index case	M	12	773	33	60											Abstinent		
		Brother	M	6	382														Abstinent	
		Father	M	35	1200															
		Grandmother	F	72	284															
		Uncle	M	45	487															
		First cousin	F	21	367															
		First cousin	M	22	584	28														
4	Belgium	Index case	M	54	1114	26														
		Daughter	F	29	263	21														
		Son	M	25	613															
		Brother	M	59	1164	28														
		Godson	M	35	1354	36														
		Goddaughter	F	32	372	25														
5	Iraq	Index case	M	71	2306	29	250	38	30	43	6		14,4		97	Fatigue	Abstinent			
6	France	Index case	M	57	1386	43		25	11	22	3	5	15,4	45,3	91	Hepatomegaly	Moderate			
		Son	M	27	1066	33														

*Age at diagnosis. **Moderate: up to 1 drink per day for women and up to 2 drinks per day for men. SF: serum ferritin (normal value ≤ 200 µg/L in females, ≤ 300 in males); TS: transferrin saturation (normal value $< 45\%$); HIC: hepatic iron concentration (normal value < 36 µmol/g); AST: aspartate aminotransferase (normal range: 5-50 IU/L); ALT: alanine aminotransferase (normal range: 5-50 IU/L); GGT: gamma-glutamyl transferase (normal range: 5-55 IU/L); CRP: C-reactive protein; RBC: red blood cell (normal range: $4.0\text{-}5.7 \times 10^{12}/L$); Hb: hemoglobin (normal range: 12.0-18.0 g/dL); Ht: hematocrit (normal range: 37-52%); MCV: mean corpuscular volume (normal range: 80-95 fL).

reported by Taniguchi *et al.* in 2015¹⁹ and, as templates, the experimental 3D structures of *Bdellovibrio bacteriovorus* (Bb) iron transporter Bd2019 in outward and inward facing conformations (pdb 5aym and 5ayo,¹⁹ respectively).

Statistical analysis

Data are presented as scatter dot plots and means. Comparisons used a one-tailed Student's *t*-test.

Results

Clinical data and segregation analysis

The *SLC40A1* p.Arg178Gln (c.533G>A) variant was identified in 22 patients from six independent families (Figure 1). It co-segregated with hyperferritinemia (defined as serum ferritin > 300 µg/L in males and > 200 µg/L in females) in all the tested patients, irrespective of age at testing, and was absent in three non-affected members of families 3 and 4.

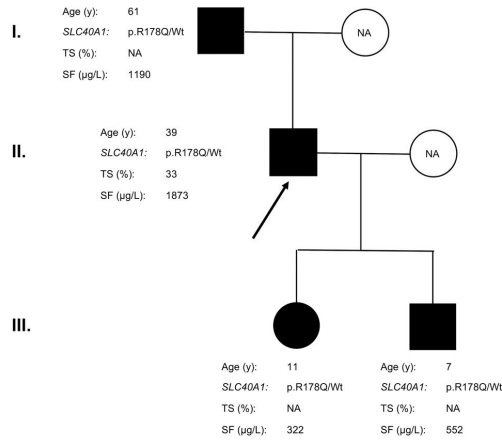
Index cases comprised six males, aged 12-72 years at diagnosis, who displayed significant hyperferritinemia and non-elevated transferrin saturation (Table 1). Hepatic Iron Concentration (HIC) was evaluated using the Gandon's magnetic resonance imaging (MRI) method²⁰ in three patients with values between 60 (youngest case) and 250 µmol/g (oldest case) dry weight. Liver biopsy, performed in the index case of family 1, confirmed iron

overload, with a predominance of iron deposition in Kupffer cells (Figure 2). The patient showed no clinical symptoms, except for persistent fatigue. The platelet count ($178 \times 10^9/L$; normal range: $120\text{-}369 \times 10^9/L$) was not suggestive of a fibrotic liver disease. The patient started a phlebotomy program. After 24 phlebotomies (450 mL every three weeks), the hemoglobin level dropped to 13.6 g/dL, from 15.7 g/dL at diagnosis (normal range: 13.5 – 17.5).

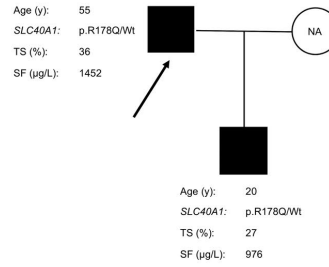
In total, the cohort consisted of 17 males and five females. Women had lower serum ferritin levels than men (263-372 versus 487-2306 µg/L), while four children exhibited increased iron store between the ages of six and 12. Carrier testing in families identified 16 patients for whom no clinical manifestations of iron overload were reported.

Serum hepcidin measurements were obtained before therapeutic phlebotomy in two affected individuals of family 3 (3.II.5 and 3.III.4). They were above the reported range in healthy individuals for the assay used (1.0-21 ng/mL; liquid chromatography coupled with tandem mass spectrometry).¹⁶ The proband's grandmother (3.I.1) started therapeutic phlebotomy (1-2 venesections per year; well tolerated) several years before family screening. She showed moderately increased ferritin (280 µg/L) at the time of serum hepcidin evaluation (41.6 ng/mL). In contrast, normal serum hepcidin levels (8.2 ng/mL) were detected in the proband's brother who was negative for

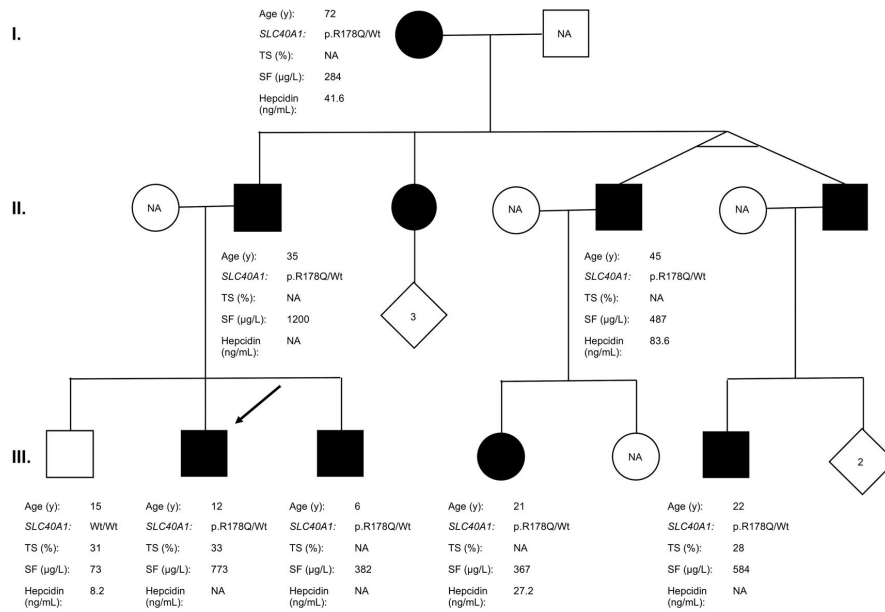
Family 1



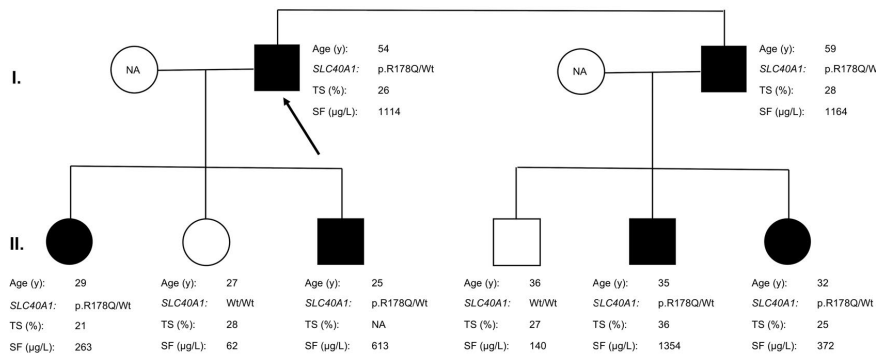
Family 2



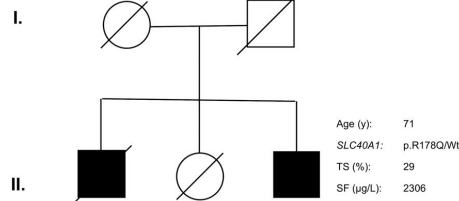
Family 3



Family 4



Family 5



Family 6

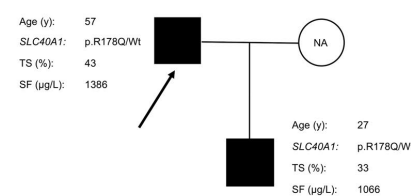


Figure 1. Family studies and pedigrees with the p.Arg178Gln missense mutation. Arrows indicate the index case. Biological data of family members are presented, when available. TS: transferrin saturation; SF: serum ferritin.

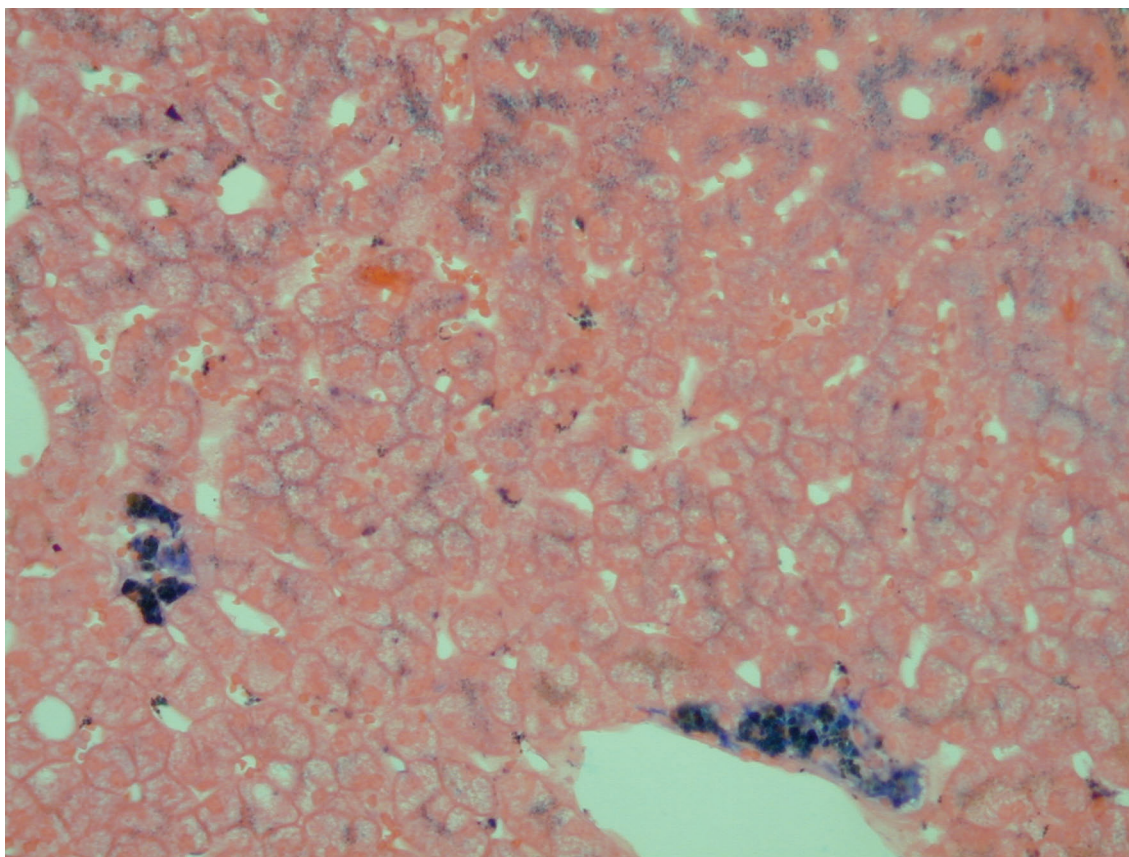


Figure 2. Liver histology of the index case of family 1 at diagnosis. Perls' stain of liver biopsy shows significant amounts of stainable iron in Kupffer macrophages, while mild iron overload is observed in hepatocytes.

the SLC40A1 p.Arg178Gln missense mutation and had normal iron indices (3.III.1).

It is noteworthy that the index case of family 2 and his son had two co-existing conditions of hyperferritinemia: hemochromatosis type 4 and hepatic steatosis. Transient Elastography-based Controlled Attenuation Parameter (TE-CAP) measurements revealed grade 3 severe steatosis in both family members (CAP scores: 396 and 363 dB/m, respectively). The index case was a 55-year-old male with 36% transferrin saturation and a serum ferritin level of 1,452 µg/L at diagnosis. He presented with a waist circumference of 104 cm, in a context of subnormal laboratory metabolic and liver tests: uric acid (453 mol/L; normal range: 240-420), total cholesterol (7 mmol/L; normal range: 3.5-6.0), alanine aminotransferase (58 IU/L; normal range: 5-50) and gamma-glutamyl transferase (61 IU/L; normal range: 5-55). Blood pressure, aspartate aminotransferase, triglycerides, HDL cholesterol and fasting blood glucose were within normal ranges. Abdominal magnetic MRI showed significantly reduced liver signal intensity, consistent with advanced iron overload (HIC: 180 µmol/g). The patient started venesection therapy when he turned 60 years old, after being diagnosed with prostate cancer and colon polyps. The phlebotomy program (500 mL every two weeks for eight months, then monthly for four months) was well tolerated. His son, who became overweight during infancy (waist circumference at diagnosis: 105 cm; Body Mass Index: 31.7 kg/m²), presented

similar iron indices at the age of 20 years (transferrin saturation: 27%; serum ferritin: 976 µg/L). MRI, however, revealed a moderate increase in hepatic iron store (HIC: 85 µmol/g).

Functional characterization of the ferroportin 1 p.Arg178Gln variant

The functional significance of the p.Arg178Gln variant was determined by first investigating its subcellular localization. Wild-type (WT) and mutant ferroportin 1-V5 constructs were expressed in HEK293T cells, and plasma membrane localization of the V5-tagged proteins was assayed by Western blot and densitometry. HLA-A was used as the control and standard for normalization, being a cell-surface protein with no known role in iron metabolism. The p.Ala77Asp missense mutation, which significantly damages ferroportin 1 structure and is known to prevent cell-surface localization,^{17,21} was used as the negative control. The p.Arg178Gln mutant was properly localized on the cell surface, comparable to the WT protein (Figure 3A).

Next, the iron-exporting function of the ferroportin 1 p.Arg178Gln variant was assessed using radioactively labeled iron. HEK293T cells were grown in 20 µg/L ⁵⁵Fe-transferrin for 24 hr, washed, transiently transfected, and placed in a serum-free medium. The amount of ⁵⁵Fe exported into the supernatant was measured after a period of 36 hr using cells transfected with the commercial

pcDNA3.1-V5-His vector as negative control (no FPN1). As shown in Figure 3B, cells transfected with WT ferroportin 1-V5 displayed a 3-fold increase in iron release. The p.Arg178Gln variant was not able to export iron ^{55}Fe in amounts comparable with WT ferroportin 1, but was more active than the p.Ala77Asp control; Student's *t*-tests highlighted significant differences between both variants and WT ferroportin 1 ($P < 0.001$ and 0.0001 , respectively) and between the two variants ($P < 0.0001$).

To investigate whether the p.Arg178Gln missense mutation could modify response to hepcidin, transiently transfected HEK293T cells were cultured for 24 hr with conditioned media derived from T-Rex-293 cells stably transfected with full-length human HAMP cDNA. Supernatant human-25 hepcidin concentration was determined using a competitive enzyme-linked immunosorbent assay. Two known ferroportin 1 mutants served as positive controls: p.Asn144His, which shows partial resistance to hepcidin inhibition,²² and p.Cys326Tyr, which abolishes hepcidin binding to ferroportin 1 and is responsible for complete resistance.²³ As expected, the addition of hepcidin to cells expressing WT ferroportin 1 resulted in the disappearance of the iron exporter from the plasma membrane. The Western blot pattern of the p.Asp178Gln variant, unlike the p.Cys326Tyr and p.Asn144His mutants, was similar to that of the WT protein (Figure 4).

Structural and functional investigation of the intermolecular interaction between the N and C lobes of human ferroportin 1 – 3D structure form I (outward facing)

In order to understand the possible impact of the p.Arg178Gln mutation, we modeled the 3D structure of human ferroportin in both the outward and inward facing conformations, based on the recent 3D structures of the Bb iron transporter Bd2019, which shares 24% sequence identity with human ferroportin 1.¹⁹

As illustrated in Figure 5, Arg178 forms an inter-lobe salt bridge with Asp473 in the outward facing conformation of human ferroportin 1. We hypothesized that this non-covalent interaction between helix TM5 and helix TM8, located respectively in the N and C lobes, might be important in stabilizing the outward facing conformation of ferroportin 1, and that its disruption might cause a significant reduction in iron egress.

To check this hypothesis, we replaced arginine 178 and aspartic acid 473 with alanine, which is the smallest amino acid after glycine and is neutral, being non-polar and devoid of any strong hydrophobic character. Moreover, it has the highest propensity of the 20 amino acids for the α -helical state;²⁴ thus this modification was likely to have limited impact on local structure. As shown in Figure 6, the Asp473Ala mutant did not cause obvious mislocalization of the protein, which was, however, totally inoperative for iron export. Indeed, cells expressing the Asp473Ala mutant retained ^{55}Fe in amounts comparable to cells expressing the two known p.Asn77Asp and p.Val162del loss-of-function mutations. The Arg178Ala mutant reduced cell surface expression to half that of the WT, but with less influence in iron export ability.

We then examined whether charge swapping could restore the iron export function of ferroportin 1, and whether Arg178Gln dysfunction could be corrected by a p.Asp473Arg mutation. The p.Arg178Asp and

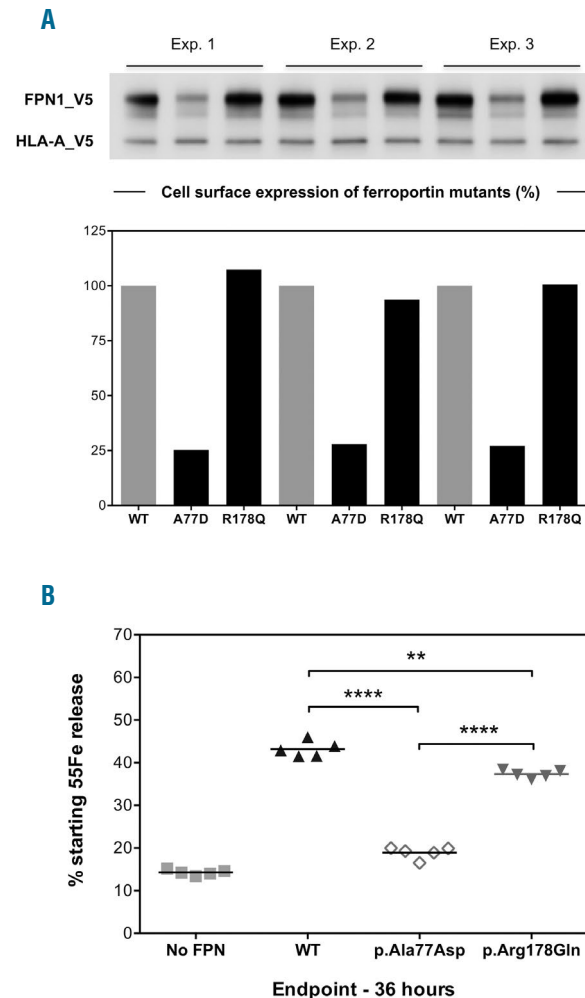


Figure 3. The ferroportin p.Arg178Gln mutant shows normal cell surface expression, but substantial loss of iron export. (A) HEK293T cells were transiently co-transfected with plasmids encoding either a V5-tagged ferroportin protein (WT or variant) or a V5-tagged HLA-A protein. Human leukocyte antigen (HLA)-A was used as control and standard for normalization, being a cell surface protein with no known role in iron metabolism. At 24h after transfection, cell surface proteins were selectively purified and analyzed by Western blotting using a peroxidase conjugated mouse anti-V5 antibody. Densitometric scans of SLC40A1 levels (normalized to HLA-A) are shown in the lower part of the figure. The results of three independent experiments are presented. (B) HEK293T cells were grown in $20 \mu\text{g/mL}$ ^{55}Fe -transferrin for 24h before being washed and transiently transfected with WT or mutated SLC40A1-V5 expression plasmids. After 15h, cells were washed and then serum-starved. The ^{55}Fe exported into the supernatant was collected at 36h. Data are presented as percentage of cellular radioactivity at time zero. Each point represents the average value (from triplicate) of five independent experiments. *P* values were calculated with the Student's *t*-test; ** $P < 0.01$ and **** $P < 0.0001$. WT: wild-type.

p.Asp473Arg substitutions almost abolished cell surface expression of the protein. Introducing the two p.Arg178Asp and p.Asp473Arg missense mutations did not rescue the membrane expression level decreased by single mutations. The Arg178Gln/Asp473Arg double mutant also resulted in a strong reduction in cell surface expression (*Online Supplementary Figure S1*).

Taken together, these results suggested that the salt bridge between arginine 178 and aspartic acid 473 is essential for ferroportin 1 iron export function. Any subtle changes in charge or size on the side chains may cause loss of function.

Discussion

The p.Arg178Gln missense mutation is typical of the ferroportin 1 variants for which evidence remains inadequate and clinical pathogenicity doubtful. Herein, we provide a comprehensive genotype-phenotype analysis, and argue

that p.Arg178Gln substitution abolishes a salt bridge between the N and C lobes of human ferroportin 1, leading to a less stable outward facing state and, thus, to an altered equilibrium between the different conformational states.

The p.Arg178Gln missense mutation was first reported in a 70-year-old female with hyperferritinemia and normal

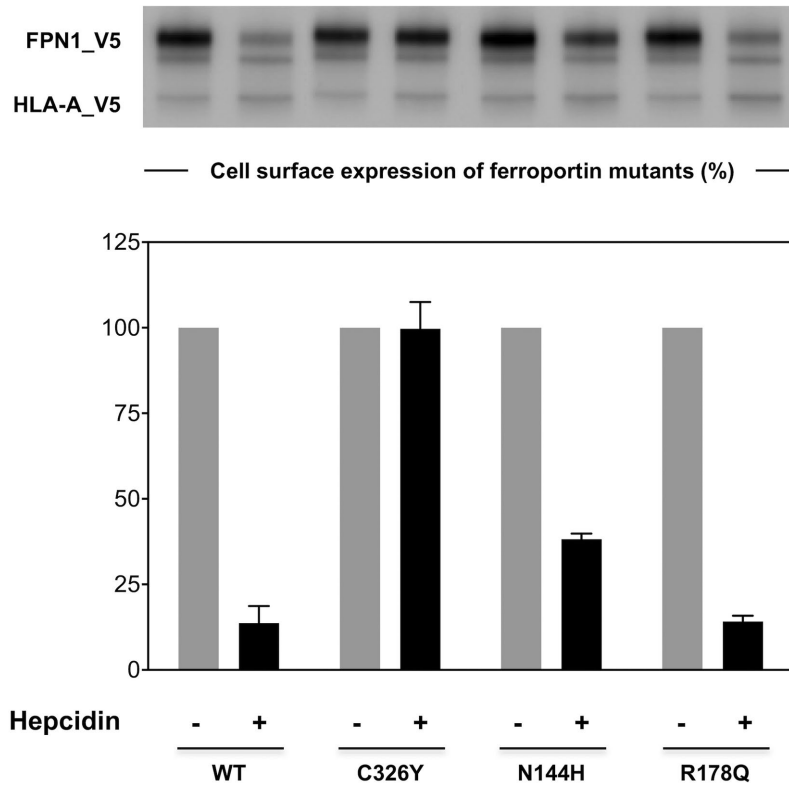


Figure 4. The ferroportin p.Arg178Gln mutant is not resistant to hepcidin. HEK293T cells were transiently co-transfected with plasmids expressing HLA(A)-V5 and either wild-type SLC40A1-V5 (WT) or SLC40A1-V5 variants. At 16h post-transfection, the cells were incubated in the presence or absence of hepcidin for 3h. Plasma membrane proteins were purified and analyzed by Western blotting and densitometry. Data are expressed as the percentage of ferroportin in cells not treated by hepcidin, according to the formula $100 \times (\text{SLC40A1} - \text{hepcidin} / \text{SLC40A1} + \text{hepcidin})$. Error bars are the standard deviation of three independent experiments.

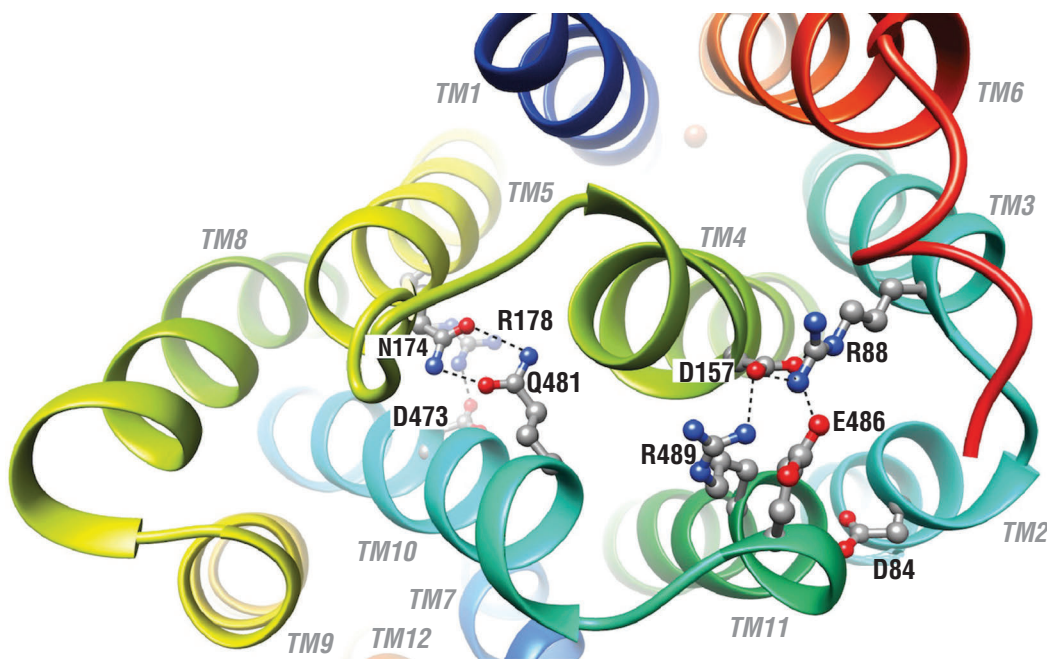


Figure 5. Ribbon representation of a human ferroportin-1 3D structure model in an outward facing conformation, with atomic representation of amino acids involved in non-covalent bonds, likely leading to the stabilization of this conformation. The iron within the iron-binding site is represented as a red ball at the top of the figure. This figure was drawn using Chimera.³⁸

transferrin saturation,²⁵ and then observed with incomplete penetrance in members of an independent Greek family. Serum ferritin was found to be markedly elevated in the proband (a 25-year-old female), but only slightly in her 53-year-old mother and within the normal range in her 87-year-old grandfather.^{26,27} We observed the p.Arg178Gln missense mutation in 11 adult males with high serum ferritin concentrations (>970 µg/L) and normal plasma iron levels (transferrin saturation: 26-43%). Three adult females from the larger pedigrees (3.III.4, 4.II.1 and 4.II.6) displayed a mild phenotype, with serum ferritin concentrations ranging between 200 and 400 µg/L at diagnosis, while two males presented an intermediate phenotype (584 and 613 µg/L) in their third decade (3.III.6 and 4.II.3). Liver biopsy was available for the index case of family 1, and showed tissue iron overload, with iron deposits primarily observed in non-parenchymal cells. The index case

had two children who exhibited increased iron stores at 11 and seven years of age, respectively. Similar phenotypes were observed in two children from family 3 (3.III.2 and 3.III.3). None of the patients were reported to have developed significant fibrosis or cirrhosis. Taken together, these data indicate that the p.Arg178Gln substitution is responsible for the classic form of ferroportin disease, or hemochromatosis type 4A. The expressivity of the *SLC40A1* p.[Arg178Gln];[=] genotype is variable, with milder phenotypes observed in women. High serum ferritin levels can be observed in young patients, highlighting the fact that tissue iron overload may appear early in life and that, in contrast to *HFE* hemochromatosis, diagnosis of ferroportin disease should not be restricted to adults.²⁸ This recapitulates some previous observations on the relationship between ferroportin loss-of-function mutations and mild to severe reticuloendothelial iron overload.^{2,11,29}

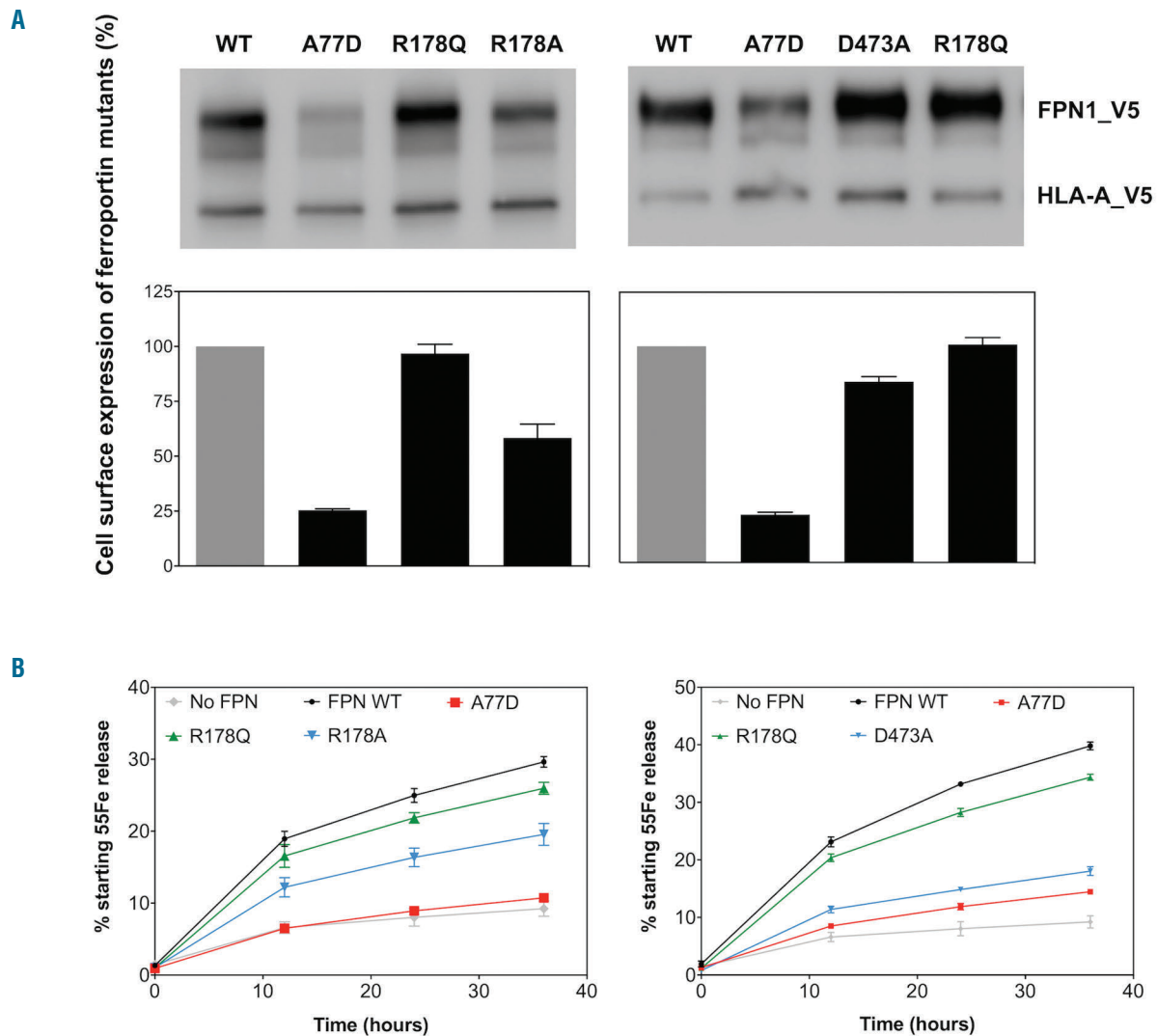


Figure 6. Effect of p.Arg178Ala and p.Asp473Ala ferroportin variants on cell surface expression and iron export. (A) HEK293T cells were transiently co-transfected with plasmids encoding either a V5-tagged ferroportin protein (WT or variant) or a V5-tagged HLA-A protein. At 24h after transfection, cell surface proteins were selectively purified and analyzed by Western blotting using peroxidase-conjugated mouse anti-V5 antibody. Densitometric scans of SLC40A1 levels (normalized to HLA-A) are shown. The error bars represent the standard deviation of three independent experiments. (B) HEK293T cells were grown in 20 µg/mL ⁵⁵Fe-transferrin for 24h before being washed and transiently transfected with WT or mutated SLC40A1-V5 expression plasmids. After 15h, cells were washed and then serum-starved for up to 36h. ⁵⁵Fe exported into the supernatant was collected at various time points. Data are presented as a percentage of cellular radioactivity at time zero. Each point represents the mean standard deviation; n=3 in each group. The data are representative of three separate experiments. WT: wild-type.

In contrast to all other types of hemochromatosis, which are characterized by hepcidin deficiency, we found increased serum hepcidin levels in three affected individuals from family 3. This recapitulates previous observations in seven patients with the recurrent and well-characterized p.Val162del loss-of-function ferroportin 1 mutation.^{11,30,31}

M. Speletas *et al.* and S. Cunat *et al.* failed to detect the p.Arg178Gln missense mutation in the DNA of 253 bone marrow donors from central Greece²⁷ and 50 French controls.²⁵ The results presented herein of 730 DNA samples from healthy subjects born in the western part of France (Brittany) were identical. The variant was also absent in GnomAD, which is an extension of the Exome Aggregation Consortium (ExAC) database and includes 123,136 exome sequences and 15,496 whole-genome sequences from unrelated individuals sequenced as part of various disease-specific and population genetic studies. The p.Arg178Gln missense mutation can thus be expected to be very rare; nevertheless, it has now been associated with hyperferritinemia in 25 patients from France, Belgium, Greece and Iraq. This provides another indication of the pathogenicity of the *SLC40A1* p.Arg178Gln allele, which is not restricted to European populations.

We and others have previously shown that the p.Arg88Gly, p.Ile152Phe and p.Asn174Ile clinical mutations are defective in terms of iron egress while being normally addressed to the cell surface.^{14,17,32,33} In the present study, we demonstrated that the p.Arg178Gln substitution follows an identical trend (Figure 3). This was not a typical situation of loss of ferroportin 1 function, which is usually associated with protein mislocalization.^{14,21} This prompted us to look at the 3D structure of human ferroportin 1 and examine the molecular mechanism responsible for reduced iron export.

Ferroportin 1 is a member of the major facilitator superfamily (MFS),¹⁷ which is the largest group of secondary active membrane transporters, essential for the movement of a wide range of substrates across biological membranes.³⁴ In recent years, the number of experimental 3D structures has increased dramatically, leading to a better appreciation of the conformational changes that are needed for effective MFS-mediated transport.^{35,36} All MFS transporters share a common and characteristic core fold that is organized in two similar domains (N and C lobes), each consisting of six consecutive transmembrane segments (TM1-TM6 and TM7-TM12). They progress through a conformational cycle that involves at least four conformational states: inward open state, the ligand-bound and ligand-free occluded states, and outward open state.³⁶ These conformational changes are orchestrated by

a set of specific residues that mediate interactions between the N and C lobes.³⁵

The recent report of the crystal structures of a putative bacterial homologue of ferroportin 1 (BbFPN) and the description of inter- and intra-domain conformational rearrangements during the transport of iron open up new avenues for predicting the atomic details of the organization of human ferroportin transmembrane helices and elucidating the detailed mechanisms of iron egress.¹⁹ Such structural investigation has already been conducted, using more distant 3D structures as a template.^{14,17,37} In the present study, we built an outward-open conformation of human ferroportin 1, using the experimental structure of BbFPN as a template. This allowed us to specifically investigate interactions between TM3, TM4 and TM5 of the N lobe and TM8 and TM9 of the C lobe (Figure 5). We demonstrated that Arg178 (TM5) forms a salt bridge with Asp473 (TM8). This bond may act in the same way as those observed between Asn174 (TM5) and Gln481 (TM10), or between Arg88 (TM3) and Glu486 (TM11) and between Asp157 (TM4) and Arg489 (TM11), thus extending the definition of an interaction network on the intracellular side of the outward facing structure of BbFPN.¹⁹ That the interaction between Arg178 and Asp473 is important in stabilizing human ferroportin 1 in the outward facing state is further supported by the results presented in Figure 6, where replacing arginine 178 or aspartic acid 473 by alanine strongly decreased the ability of ferroportin 1 to export iron. The reason why the Asp473Ala mutant showed a smaller impact on protein trafficking than Arg178Ala, despite its stronger effect on iron egress, remains to be elucidated. One possibility is that the interruption of the charge-helix dipole interaction (Arg178 – Asp 181) may destabilize the local structure of TM3.

To conclude, the present study demonstrates the causality of the p.Arg178Gln missense mutation, which is now considered to be one of the most frequent *SLC40A1* loss-of-function mutations. It also reveals a new molecular mechanism of disease, involving residues that participate in the stabilization of the different conformational states and thus mediate iron export. These findings can be extended to the functional interpretation of other rare missense mutations that are associated with typical reticuloendothelial iron overload but do not significantly alter the cell surface expression of ferroportin 1. They also confirm that it is essential to identify so-called “gating residues” in order to fully understand the action mechanism of MFS transporters.³⁵

Funding

The authors would like to thank the French Hospital Clinical Research Program (Programme Hospitalier de Recherche Clinique 2009) for funding; Brest University Hospital UF0857.

References

- Wallace DF, Subramaniam VN. The global prevalence of HFE and non-HFE hemochromatosis estimated from analysis of next-generation sequencing data. *Genet Med.* 2016;18(6):618-626.
- Pietrangelo A. Ferroportin disease: pathogenesis, diagnosis and treatment. *Haematologica.* 2017;102(12):1972-1984.
- Donovan A, Lima CA, Pinkus JL, et al. The iron exporter ferroportin/Slc40a1 is essential for iron homeostasis. *Cell Metab.* 2005; 1(3):191-200.
- Drakesmith H, Nemeth E, Ganz T. Ironing out ferroportin. *Cell Metab.* 2015; 22(5):777-787.
- Girelli D, Nemeth E, Swinkels DW. Hepcidin in the diagnosis of iron disorders. *Blood.* 2016;127(23):2809-2813.
- Ganz T. Macrophages and iron metabolism. *Microbiol Spectr.* 2016;4(5).
- Pietrangelo A. The ferroportin disease. *Blood Cells Mol Dis.* 2004;32(1):131-138.
- Cremonesi L, Cemonesi L, Forni GL, et al. Genetic and clinical heterogeneity of ferroportin disease. *Br J Haematol.* 2005; 131(5):663-670.
- Pietrangelo A, Montosi G, Totaro A, et al. Hereditary hemochromatosis in adults

- without pathogenic mutations in the hemochromatosis gene. *N Engl J Med*. 1999;341(10):725-732.
10. McDonald CJ, Wallace DF, Ostini L, Bell SJ, Demediuk B, Subramaniam VN. G80S-linked ferroportin disease: classical ferroportin disease in an Asian family and reclassification of the mutant as iron transport defective. *J Hepatol*. 2011;54(3):538-544.
 11. Mayr R, Janecke AR, Schranz M, et al. Ferroportin disease: a systematic meta-analysis of clinical and molecular findings. *J Hepatol*. 2010;53(5):941-949.
 12. MacArthur DG, Manolio TA, Dimmock DP, et al. Guidelines for investigating causality of sequence variants in human disease. *Nature*. 2014;508(7497):469-476.
 13. Richards S, Aziz N, Bale S, et al. Standards and guidelines for the interpretation of sequence variants: a joint consensus recommendation of the American College of Medical Genetics and Genomics and the Association for Molecular Pathology. *Genet Med*. 2015;17(5):405-424.
 14. Callebaut I, Joubrel R, Pissard S, et al. Comprehensive functional annotation of 18 missense mutations found in suspected hemochromatosis type 4 patients. *Hum Mol Genet*. 2014;23(17):4479-4490.
 15. Adams PC, Barton JC. A diagnostic approach to hyperferritinemia with a non-elevated transferrin saturation. *J Hepatol*. 2011;55(2):453-458.
 16. Lefebvre T, Dessendier N, Houamel D, et al. LC-MS/MS method for hepcidin-25 measurement in human and mouse serum: clinical and research implications in iron disorders. *Clin Chem Lab Med*. 2015; 53(10):1557-1567.
 17. Le Gac G, Ka C, Joubrel R, et al. Structure-function analysis of the human ferroportin iron exporter (SLC40A1): effect of hemochromatosis type 4 disease mutations and identification of critical residues. *Hum Mutat*. 2013;34(10):1371-1380.
 18. Martí-Renom MA, Stuart AC, Fiser A, Sánchez R, Melo F, Sali A. Comparative protein structure modeling of genes and genomes. *Annu Rev Biophys Biomol Struct*. 2000;29:291-325.
 19. Taniguchi R, Kato HE, Font J, et al. Outward- and inward-facing structures of a putative bacterial transition-metal transporter with homology to ferroportin. *Nat Commun*. 2015;6:8545.
 20. Gandon Y, Olivie D, Guyader D, et al. Non-invasive assessment of hepatic iron stores by MRI. *Lancet*. 2004;363(9406):357-362.
 21. Schimanski LM, Drakesmith H, Merryweather-Clarke AT, et al. In vitro functional analysis of human ferroportin (FPN) and hemochromatosis-associated FPN mutations. *Blood*. 2005;105(10):4096-4102.
 22. Drakesmith H, Schimanski LM, Ormerod E, et al. Resistance to hepcidin is conferred by hemochromatosis-associated mutations of ferroportin. *Blood*. 2005;106(3):1092-1097.
 23. Fernandes A, Preza GC, Phung Y, et al. The molecular basis of hepcidin-resistant hereditary hemochromatosis. *Blood*. 2009; 114(2):437-443.
 24. Callebaut I, Labesse G, Durand P, et al. Deciphering protein sequence information through hydrophobic cluster analysis (HCA): current status and perspectives. *Cell Mol Life Sci*. 1997;53(8):621-645.
 25. Cunat S, Giansily-Blaizot M, Bismuth M, et al. Global sequencing approach for characterizing the molecular background of hereditary iron disorders. *Clin Chem*. 2007; 53(12):2060-2069.
 26. Speletas M, Kioumi A, Loules G, et al. Analysis of SLC40A1 gene at the mRNA level reveals rapidly the causative mutations in patients with hereditary hemochromatosis type IV. *Blood Cells Mol Dis*. 2008;40(3):353-359.
 27. Speletas M, Onoufriadis E, Kioumi A, Gemenis AE. SLC40A1-R178G mutation and ferroportin disease. *J Hepatol*. 2011;55(3):730-731; author reply 731-732.
 28. Galicia-Poblet G, Cid-Paris E, López-Andrés N, et al. Pediatric ferroportin disease. *J Pediatr Gastroenterol Nutr*. 2016; 63(6):e205-e207.
 29. Le Lan C, Mosser A, Ropert M, et al. Sex and acquired cofactors determine phenotypes of ferroportin disease. 2011;140(4):1199-1207.e2.
 30. Papanikolaou G, Tzilianos M, Christakis JJ, et al. Hepcidin in iron overload disorders. *Blood*. 2005;105(10):4103-4105.
 31. Zoller H, McFarlane I, Theurl I, et al. Primary iron overload with inappropriate hepcidin expression in V162del ferroportin disease. *Hepatology*. 2005;42(2):466-472.
 32. Girelli D, De Domenico I, Bozzini C, et al. Clinical, pathological, and molecular correlates in ferroportin disease: a study of two novel mutations. *J Hepatol*. 2008;49(4):664-671.
 33. De Domenico I, McVey Ward D, Nemeth E, et al. Molecular and clinical correlates in iron overload associated with mutations in ferroportin. *Haematologica*. 2006; 91(8):1092-1095.
 34. Law CJ, Maloney PC, Wang D-N. Ins and outs of major facilitator superfamily antiporters. *Annu Rev Microbiol*. 2008; 62:289-305.
 35. Quistgaard EM, Löw C, Guettou F, Nordlund P. Understanding transport by the major facilitator superfamily (MFS): structures pave the way. *Nat Rev Mol Cell Biol*. 2016;17(2):123-132.
 36. Yan N. Structural biology of the major facilitator superfamily transporters. *Annu Rev Biophys*. 2015;44:257-283.
 37. Bonaccorsi di Patti MC, Polticelli F, Cece G, et al. A structural model of human ferroportin and of its iron binding site. *FEBS J* 2014;281(12):2851-2860.
 38. Pettersen EF, Goddard TD, Huang CC, et al. UCSF Chimera—a visualization system for exploratory research and analysis. *J Comput Chem*. 2004;25(13):1605-1612.